Adsorption (2013) 19:291–304
DOI 10.1007/s10450-012-9452-9

Effects of melting and ordering on the isosteric heat and monolayer density of argon adsorption on graphite

Eugene A. Ustinov · Duong D. Do

Received: 13 October 2012 / Accepted: 6 December 2012 / Published online: 18 December 2012

Abstract The aim of this paper is to study the effects of temperature on the state of the adsorbed argon on an uniform graphite surface. We applied the kinetic Monte Carlo scheme to simulate adsorption over a very wide range of temperature, which allows us to model the vapor–solid, the vapor–liquid and the order–disorder transition of the monolayer. The main distinction of our methodology is that it accounts for the lattice constant change with loading in the case of formation of an ordered molecular layer by appropriately changing the simulation box size. To do this we enforced the equality of the tangential pressures obtained by the virial and thermodynamic routes, which corresponds to the minimum Helmholtz free energy of a system at a given number of molecules and volume. This criterion is a consequence of the Gibbs–Duhem equation. A significant result obtained by application of the new simulation method was a sharp contraction of the monolayer just after its completion and the onset of the second layer. It manifests itself in an additional heat release. We re-determined the 2D-melting and 2D-critical temperatures of the molecular layer of argon. We also analyzed the order–disorder transition above the 2D-melting and showed that it could occur at some temperatures above the 2D-critical temperature. In this case, a hexagonal lattice appears at a sufficiently large tangential pressure. The effects of loading on the lattice constant, the 2D-critical temperature of the order–disorder transition and the differential heat of adsorption are thoroughly discussed.

E.A. Ustinov (✉)
Ioffe Physical Technical Institute, 26 Polytechnicheskaya,
St. Petersburg 194021, Russia
e-mail: eustinov@mail.wplus.net

D.D. Do
School of Chemical Engineering, University of Queensland,
St. Lucia, QLD 4021, Australia

Keywords Kinetic Monte Carlo · Adsorption on graphite · Monolayer phase transition · Heat of adsorption

1 Introduction

Molecular simulation methods have been constant refined and improved, and this motivates a surge of interest to reconsider simple systems, which, in spite of their simplicity, show some discrepancy between the theoretical predictions and the experimental data. A classic example to this is the existence of a heat spike on the heat curve versus loading in the system Ar–graphite at 77 K (Rouquerol et al. 1977; Grillet et al. 1979) at a loading close to the monolayer concentration; the spike corresponds to a two-dimensional (2D) ordering transition. Reproducing of this spike by molecular simulation has been a very challenging task. There were several attempts to describe this phenomenon with grand canonical Monte Carlo method (GCMC) (Nicholson et al. 1977; Nicholson and Parsonage 1986; Wongkoblap and Do 2007; Fan et al. 2010), but they were not successful due to the apparent lack of accuracy, arising from the significant fluctuation at loadings where the heat spike occurs. A better description of this phenomenon were recently obtained with a Bin-GCMC (Fan et al. 2012). A number of works have been devoted to the 2D melting transition of simple gases adsorbed on graphite (Thomy and Duval 1970; Migone et al. 1984; Zhu and Dash 1986; Morrison 1987; Pettersen et al. 1989; D'Amico et al. 1990; Day et al. 1993; Larese and Zhang 1995; Kuchta and Etters 1987; Golebiowska et al. 2009), and it is well established that the melting temperature of argon monolayer is around 50 K. Theoretically, Abraham (1981) obtained 53.3 K for the melting point of 2D Lennard–Jones fluid using the isobaric–isothermal Monte Carlo scheme. For the 2D-critical temperature of argon monolayer a range of 55–68 K has been

reported in the literature. It is generally accepted that the 2D vapor–solid transition of the adsorbed monolayer occurs below the 2D melting temperature of 50 K, and the 2D vapor–liquid transition is in the temperature range between 50 and 65 K. The ordering transition, however, can occur even at temperatures higher than the 2D-critical temperature. For this reason, it is important to distinguish ordering transition from melting. The latter can be referred to a binary gas–solid system in which the solid phase melts and transforms into the liquid phase, while the former case is observed in a homogeneous liquid-like phase or hypercritical compressed fluid when a sufficiently large pressure forces molecules to rearrange into a crystal-like structure in order to reduce volume of the unit cell and, as a consequence, to decrease the free energy.

In our recent works (Ustinov and Do 2012a, 2012b) we have shown that in the case of an ordered molecular layer the lattice constant significantly changes with loading. This means that using a simulation cell of constant size leads to an incorrect adsorption isotherm and all thermodynamic functions because of the artifact of domains if the lattice constant is not chosen correctly. Thus, the tangential pressure determined with the virial route can deviate as much as 100 % from that determined thermodynamically. Moreover, the tangential pressure of the adsorbed phase obtained by the virial route exhibits the incorrect behavior of decreasing with loading when the ordered molecular layer has been formed; this behavior is thermodynamically impossible because the system would be mechanically unstable. To achieve the correct thermodynamic solution the "true" lattice constant at a given loading is the one that yields equality of the virial and the 'thermodynamic' pressures (Ustinov and Do 2012b). With this criterion, the lattice constant decreases with loading, and we were able to determine correctly the isotherm of argon adsorption on graphite at 77 K and the isosteric heat of adsorption. The present study is to extend our previous work to lower temperatures to identify the 2D critical and triple points and analyze the behavior of the 2D crystalline phase. There is a number of experimental and theoretical works on this topic, which are devoted to study the effects resulting from the surface corrugation of graphite. It was found, for example, that the surface corrugation increases the melting temperature by about 2 K and there is a rotational transition of the crystal-like argon adlayer relative to the substrate lattice below the melting point by 2 K (Migone et al. 1984; Flenner and Etters 2002, 2006). This is reflected in the two heat capacity peaks observed experimentally and they are reproduced in numerical simulations. However, at present we do not pursue the exact reproduction of experimental data on the behavior of argon adsorbed on graphite in order to elucidate the effects of loading and temperature on the lattice constant of the ordered monolayer, the ordering transition and the heat of adsorption. On the other hand, the lattice constant is strongly affected by the simulation box size and therefore it is necessary to have a thermodynamic criterion to make a correct choice of the box size to get consistent results of simulation. This is a fundamental problem which has not been addressed in the literature. For this reason, in the present study we neglect the periodic modulation of the argon–graphite potential to avoid any interference of secondary order effects. Such a statement can be considered as a basis for further analysis of adsorbed systems in more detail.

We used the kinetic Monte Carlo (kMC) method, which was successfully applied to equilibrium systems (Ustinov and Do 2012b), and it has been proved to be very effective owing to its advantages over the conventional Metropolis algorithm, such as the absence of discarded trial moves and the determination of chemical potential is inherent in the course of the simulation, instead of recourse to an additional step (Widom method) which requires the freezing of a configuration in the conventional MC simulation, followed by the insertion of ghost particles. This would add to the computation overhead. Therefore, another aim of this study is to validate application of the kMC to equilibrium adsorption systems.

2 Theory and methodology

All calculations presented in this work were performed with the kinetic Monte Carlo scheme, which was adapted to equilibrium systems in our previous works (Ustinov and Do 2012a, 2012b, 2012c, 2012d). We have considered the vapor–liquid equilibrium, argon adsorption and monolayer ordering transition on graphite at temperatures above the 2D critical point, and argon adsorption in slit pores at 77 and 87.3 K. In the latter case we used a canonical and grand canonical versions of kMC, which we proposed for the first time in the literature (Ustinov and Do 2012d). In this study we will focus on argon adsorption on a graphite surface over a wide range of temperature to study in details the co-existence of two phases of the adsorbed layer, including the 2D gas–solid, gas–liquid and order–disorder transition in the first molecular layer. As far as we are aware of, this is the first simulation paper dealing with these phenomena and the evolution of phase equilibria as temperature is increased from below the 2D triple point to above the 2D-critical point of the monolayer.

Simulations were mainly carried out in a rectangular cell having dimensions L_x, L_z of $23\sigma_{ff}$ and $10\sigma_{ff}$ along the x and z directions, respectively. The dimension L_y was set equal to $L_x\sqrt{3}/2$ to ensure the conformity of the hexagonal lattice whose one of its symmetry axes is directed along the x direction. In order to use the conventional periodic boundary conditions it is necessary that the number of unit cells

(row) along the y direction is even. In this work the number of rows was 20 and the number of perfect hexagonal lattices in the XY plane was 400.

The Lennard–Jones parameters for argon have been precisely determined in the framework of kMC applied to the vapor–liquid interface over a wide range of temperature to reproduce the heat of evaporation, the surface tension, the saturation pressure and the densities of the coexisting phases (Ustinov and Do 2012c). The collision diameter σ_{ff} and the potential well depth ε_{ff}/k_B are close to the commonly used values and equal to 0.3393 nm and 118.4 K, respectively. For the solid–fluid potential we used a structureless model of graphite with the LJ parameters determined by the Lorentz–Berthelot mixing rule, with the molecular parameters for a carbon atom in the graphene layer being 0.34 nm and 28 K for the collision diameter σ_{ss} and the potential well depth ε_{ss}/k_B, respectively. The chemical potential and the tangential pressure were calculated according to prescriptions described previously (Ustinov and Do 2012a, 2012b). It should be noted that in the general case there is a difference between the virial pressure calculated with the Irving–Kirkwood equation (Irving and Kirkwood 1950) and the thermodynamic pressure determined as the difference between the Gibbs and Helmholtz free energies of the system over its volume, which is the tangential pressure in the case of gas adsorption on a flat smooth surface of infinite extent (Ustinov and Do 2012d). The difference between the 'virial' and 'thermodynamic' tangential pressures arises in those cases where we have a 2D crystalline structure of the molecular layer and the lattice constant is governed by the dimensions of the simulation cell. As is shown in our previous work (Ustinov and Do 2012b), the minimum of the Helmholtz free energy corresponds to the lattice constant that yields the equality of the virial and thermodynamic pressures. What this means is that the dimensions of the simulation box cannot be chosen arbitrarily; otherwise, once the 2D crystalline lattice has been formed, the simulated adsorption isotherm, the heat of adsorption and the thermodynamic functions would be erroneous and even unphysical because at a constant size of the simulation box the pressure determined with the virial route decreases with an increase of the chemical potential. Such a behavior is typical only for unstable systems, whilst the real system under consideration is thermodynamically stable. A method of determination of the lattice constant at various loadings was based on the analysis of a family of adsorption isotherms simulated with boxes of different dimensions. Given these results we search for the lattice constant and consequently the amount adsorbed such that the 'thermodynamic' pressure is the same as the 'virial' pressure. This point corresponds to the infinitely large equilibrium system. This prescription allows us to obtain the dependence of the lattice constant on loading, which consequently yields the correct simulation results of isotherms and other thermodynamic properties. However, such a technique is rather involved and requires too many simulation runs. For this reason, in this study we used an alternative procedure, which is described below.

2.1 Effect of loading on the lattice constant

At a given temperature and number of molecules j ($> j_m$, where j_m is the number of molecules required to form a completed 2D crystalline layer) one can determine the 'thermodynamic' tangential pressure p_T and the 'virial' tangential pressure p'_T. Generally, $p_T \neq p'_T$, but we can make them equal by varying the box volume V keeping the same the box length L_z and the ratio $L_y/L_x = \sqrt{3}/2$. Suppose that $p_T = p'_T$ at a given values of j and $V = V_j$. In this case the Helmholtz free energy F_j is the difference of the Gibbs free energy $G_j = j\mu_j$ and the product $p_{T_j}V_j$, i.e.

$$F_j = j\mu_j - p_{T_j}V_j \tag{1}$$

The question is how the volume V must change after adding a molecule to the system to keep the above equality of pressures. Since the Helmholtz free energy is the integral of the chemical potential with respect to number of molecules at a constant volume, the addition one molecule to the system at the same volume V_j changes the Helmholtz free energy approximately by $(\mu_{j+1} + \mu_j)/2$. Further change of the volume at constant number of molecules changes the Helmholtz free energy by $(V_{j+1} - V_j)(p'_{T_{j+1}} + p'_{T_j})/2$. The resulting change of the Helmholtz free energy is

$$F_{j+1} - F_j = \frac{1}{2}(\mu_{j+1} + \mu_j) - \frac{1}{2}\left(p'_{T_{j+1}} + p'_{T_j}\right)(V_{j+1} - V_j) \tag{2}$$

To retain the thermodynamic consistency it is necessary that

$$F_{j+1} = (j+1)\mu_{j+1} - p_{T_{j+1}}V_{j+1} \tag{3}$$

Substitution of F_j and F_{j+1} from (1) and (3) to (2) and accounting for $p_{T_{j+1}} = p'_{T_{j+1}}$ yields, after simplifications:

$$\left(j + \frac{1}{2}\right)(\mu_{j+1} - \mu_j) \cong \frac{1}{2}(V_{j+1} + V_j)\left(p'_{T_{j+1}} - p'_{T_j}\right) \tag{4}$$

It is easily seen that if the number of molecules j is sufficiently large, the above equation transforms into the Gibbs–Duhem equation:

$$j d\mu = V dp_T \tag{5}$$

Therefore, if the simulation box size affects the properties of the adsorbed phase, which is always observed in the case of formation of an ordered molecular layer, the system must

obey the Gibbs–Duhem equation to ensure its thermodynamic consistency. This means that the size of the simulation box has to be adjusted at each loading to ensure that the Gibbs–Duhem equation is obeyed. Equation (4) is our working equation for this purpose. Once the values V_j, μ_j, and p'_{T_j} are known for j molecules, the next value V_{j+1} after adding one new molecule to the system is determined during equilibration stage so that the equality (4) is valid. Having adjusted the box volume, the length L_x was determined easily using the constant ratio L_y/L_x.

It should be noted that the tangential pressure in (1) to (5) is the average value of the 3D pressure acting on the lateral surface of the simulation box. This is because the average tangential pressure times the volume change at constant L_z length is the negative change in the Helmholtz free energy. Naturally, the average tangential pressure depends on L_z, but the product $p_T V$ does not. Therefore, the choice of the height of the simulation box can be arbitrary.

2.2 Smoothing, averaging and differentiation

In order to suppress fluctuations in the simulation we used the grand canonical partition function (Hansen and McDonald 1986):

$$\Xi(T, V, \mu) = \sum_j \exp\left(j\frac{\mu}{k_B T} - \frac{F_j}{k_B T}\right) \tag{6}$$

Each term in the sum of the right hand side (RHS) is proportional to the probability that j molecules will be found in the system and the grand canonical potential Ω is given by

$$\Omega = -k_B T \ln \Xi \tag{7}$$

The Helmholtz free energy F_j of the system with j molecules is the integral of the chemical potential μ over the number of molecules (in macroscopic systems j can be treated as a continuous variable), which can be replaced without a significant loss of accuracy by the following sum:

$$F_j = \int_0^j \mu di \cong \sum_{i=1}^{j} \mu_i \tag{8}$$

The set of values of the chemical potential μ_i can be determined with the canonical kMC for each system containing i molecules. For a given temperature T and a chemical potential μ and the set Helmholtz free energies in Eq. (8) obtained from a family of canonical kMC simulation, we can calculate the average number of molecules in an ensemble of open systems as follows:

$$\langle j \rangle = \frac{\sum_i i \exp[(i\mu - F_i)/(k_B T)]}{\sum_i \exp[(i\mu - F_i)/(k_B T)]} \tag{9}$$

Equation (9) is the expression for the thermodynamically equilibrium adsorption isotherm, which represents a dependence of amount adsorbed (in terms of number of molecules) on the chemical potential at a specified temperature. If the isotherm is a monotonic function, (9) presents a smoothed adsorption isotherm obtained in a canonical ensemble. The effect of smoothing is provided by the fact that the average $\langle j \rangle$ at a given T and μ is governed by several terms in the numerator and the denominator in the neighborhood of $\langle j \rangle$ whose the exponent passes through its maximum. If the adsorption isotherm simulated in a canonical ensemble is not monotonically increasing with the chemical potential, (9) will yield a more or less sharp transition in the region where the canonical isotherm exhibits an unstable behavior of a decrease of the chemical potential with the amount adsorbed. If the systems of the ensemble are macroscopic (which makes them statistically independent), the transition is a stepwise function. However, in numerical experiments the system usually contains a relatively small number of molecules, and for this reason, the transition occurs within a finite range of the chemical potential and the slope of this phase transition increases with the simulation box size, but never becomes vertical. Nevertheless, Eq. (9) is exact for the ensemble of open non-macroscopic systems and the position of phase transition can be approximately associated with the inflection point of amount adsorbed versus chemical potential.

The averaging as presented in Eq. (9) can be used to derive any thermodynamic functions, for example the average internal energy can be calculated as follows:

$$\langle U_j \rangle = \langle j u_j \rangle = \frac{\sum_i i u_i \exp[(i\mu - F_i)/(k_B T)]}{\sum_i \exp[(i\mu - F_i)/(k_B T)]} \tag{10}$$

where u_i is the molecular internal energy (including the gas–solid potential) for the system of i molecules.

Given the expressions for the average number of particle and the average internal energy, we can derive their derivatives with respect to the chemical potential, as shown below:

$$\begin{cases} \dfrac{\partial \langle j \rangle}{\partial \mu} = \dfrac{\langle j^2 \rangle - \langle j \rangle^2}{k_B T} \\ \dfrac{\partial \langle U_j \rangle}{\partial \mu} = \dfrac{\langle j^2 u_j \rangle - \langle j \rangle \langle j u_j \rangle}{k_B T} \end{cases} \tag{11}$$

from which we can find the change of the average internal energy with respect to the change in the average number of particle,

$$\frac{\partial \langle U_j \rangle}{\partial \langle j \rangle} = \frac{\langle j^2 u_j \rangle - \langle j \rangle \langle j u_j \rangle}{\langle j^2 \rangle - \langle j \rangle^2} \tag{12}$$

The isosteric heat of adsorption can be now written as (Ustinov and Do 2012a)

$$q_{st} = -\frac{\partial\langle U_j\rangle}{\partial\langle j\rangle} + u_g^p + \frac{p}{\rho} \tag{13}$$

The technique described in this section can also be used if the simulation box size changes from point to point. In this case it is necessary to reduce the simulated adsorption isotherm to a specified volume of the box. The number of molecules in the system will change proportionally to the change of the volume. Then all parameters such as the Helmholtz free energy, chemical potential, tangential pressure and the internal energy can be corrected for the set of integer number of molecules by interpolation.

2.3 'Thermodynamic' and 'mechanical' pressure in the adsorbed phase

It was shown in our previous work (Ustinov and Do 2012a) that the difference between the Gibbs and Helmholtz free energies over the volume of the system defines the tangential component of the pressure tensor in the adsorbed phase, i.e. $(G - F)/V$. Thus, for j molecules in the system $G = j\mu_j$ and accounting for Eq. (8) for the Helmholtz free energy, one can obtain:

$$p_T = V^{-1}\left[j\mu_j - \sum_{i=1}^{j} \mu_i \right] \tag{14}$$

However, this expression gives rather noisy tangential pressure due to the fluctuations of the chemical potential determined in a canonical ensemble. Application of the partition function (6) allows us to suppress the fluctuations as follows. First, instead of using the value μ_j one can use its replacement as the root of (9) by setting $\langle j\rangle = j$. By doing this, the replacement chemical potential is the smoothed chemical potential of the smoothed adsorption isotherm (9) at the loading j. This ensures much more reliable value of the chemical potential. Second, the Helmholtz free energy can be defined as the integral of μ with respect to number of molecules. Again, using (9) one can obtain:

$$F_j^{GC} = j\mu - k_B T \ln \sum_i \exp\left(\frac{i\mu - F_i}{k_B T}\right) \tag{15}$$

In order to distinguish the Helmholtz free energy corresponding to the grand canonical distribution from that simulated in a canonical ensemble with Eq. (8) we use the superscript '*GC*' at the Helmholtz free energy in the left hand side (LHS) of (15). Since $j\mu = G$, one can derive another expression for the tangential pressure as follows:

$$p_T(j) = \frac{k_B T}{V} \ln \sum_i \exp\left(\frac{i\mu - F_i}{k_B T}\right) \tag{16}$$

It should be noted again that Eqs. (14) and (16) define the tangential pressure averaged over the distance z normal to the surface of the adsorbent.

The 'mechanical' tangential pressure averaged over the z direction of the simulation box can be calculated with the Irving–Kirkwood prescription (1950), which gives

$$p'_T(j) = \frac{jk_B T}{V} - \frac{1}{S_{xy}}\left\langle \sum_{i=1}^{j-1} \sum_{k=i+1}^{j} \frac{x_{ik}^2 + y_{ik}^2}{2r_{ik}} \frac{d\varphi_{ik}}{dr_{ik}} \right\rangle \tag{17}$$

Here S_{xy} is the area of the simulation box in the XY plane parallel to the surface; x_{ik}, y_{ik} are projections of the separation distance r_{ik} between molecules i and k onto the corresponding axes; ϕ_{ik} is the Lennard–Jones potential of molecules i and k. In order to diminish the effect of fluctuations on the tangential pressure determined by the virial route one can also use the averaging procedure with the grand canonical partition function:

$$\left\langle p'_T \right\rangle_j = \frac{\sum_i p'_T(i) \exp[(i\mu - F_i)/(k_B T)}{\sum_i \exp[(i\mu - F_i)/(k_B T)} \tag{18}$$

where the chemical potential μ corresponds to the average number of molecules $\langle j\rangle = j$ according to (9).

2.4 Change of the lattice constant in the 2D gas–solid equilibrium

Below the 2D triple point the gas–solid equilibrium can be modeled with relative ease because of a significant difference in the 2D density of coexisting phases. To this end we used an elongated rectangular box along the X axis, with the ratio L_y/L_x being kept constant and equal to $\sqrt{3}/4$. The solid phase was kept in the center of the X direction by keeping the center of mass at the center of the box. The tangential pressure determined separately for the gas phase and the solid phase via the virial route. Since the system is in equilibrium and there are no potential barrier between coexisting phases the chemical potential and the tangential pressure must be the same in both phases. The equality of the chemical potential is achieved automatically, but the tangential pressure can be different depending on the box size along the Y direction. If the dimension L_y is chosen incorrectly, the lattice would be asymmetric and the components of the tangential pressure along the X and Y directions would be different. Thus, if the dimension L_y is underestimated, the Y component of the pressure will be overestimated, resulting in a higher value of the tangential pressure in the solid phase than that in the gas phase. Therefore a comparison of the pressures in the coexisting phases allows for adjusting dimension L_y of the simulation box and, consequently, determination the lattice constant of the solid phase. Practically, during the equilibration stage the L_y length was decreased or increased by $0.002\sigma_{ff}$ in each 1×10^6 MC steps

depending on whether the virial tangential pressure in the solid phase was less or greater than that in the gas phase. One symmetry axis of the hexagonal lattice was kept parallel to the Y direction, so the length L_y was always equal to an integer number of the lattice constant. We used this scheme to determine the effects of temperature on the lattice constant.

2.5 Determination of the 2D triple point

The triple point was determined by following the change in density of the condensed phase with temperature. We used an elongated box along the X direction to model the gas–solid equilibrium as described in Sect. 2.4. The sharp change in the density of the condensed phase will occur at the 2D-triple point.

2.6 Two-dimensional critical temperature

For temperatures above the 2D-triple point we modeled the 2D gas–liquid equilibrium. As the temperature approaches the 2D-critical point the region of the gas–liquid interface rapidly expands. For this reason, we proposed an alternative method, whose idea is based on the fact that the vapor–liquid phase transition is observed only when the adsorption isotherm simulated in a canonical ensemble has an unstable region where the increase of loading is accompanied by a decrease in the chemical potential. Therefore, one can assume that the temperature at which the unstable region disappears corresponds to the 2D-critical temperature. Below this point, adsorption isotherms were obtained by Eq. (9) and this allows us to construct equilibrium adsorption isotherms for an ensemble of open systems, which are replica of the system (essentially non-macroscopic) modeled in the simulation box. Each such isotherm has a sharp (but not vertical) phase transition step, which by extrapolation intersects the canonical adsorption isotherm at two points. The lower and higher points correspond to the coexisting gas-like and liquid-like phases, respectively.

3 Results and discussion

3.1 Gas–solid transition of argon in the adsorbed monolayer

We performed simulations in an elongated rectangular box with the ratio $L_y/L_x = \sqrt{3}/4$, with L_x dimension initially set to $36\sigma_{ff}$. The L_z dimension was kept constant at $10\sigma_{ff}$. The center of mass was kept at the mid-point of the L_x length as follows. If the center of mass (COM) is shifted to the left from the middle point, a molecule is inserted at a random position in the right half of the box in the next MC step, and the insertion is done in the left half if the COM is shifted to the right. Such a method allows the symmetry of the density distribution plot to remain at the center of the box, and also by doing this molecules are not shifted during the process of maintaining the center of mass at the middle of the box, avoiding the horizontal tracking of positions of all molecules if all molecules were to translate to keep the center of mass at the middle of the box.

The number of molecules in the box was chosen to fill half of the XY surface in 2D solid configuration, and they occupy the central half of the XY surface. The statistical analysis was done in the region $-1/8L_x < x < 1/8L_x$ for the solid phase and in the regions $-1/2L_x < x < -3/8L_x$ and $3/8L_x < x < 1/2L_x$ for the gas phase. The area for each phase that we used for statistical analysis was $1/4$ of the area of the XY surface, and the density distributions in those regions were presumably uniform, which would be confirmed after the analysis.

One of the symmetry axes of the hexagonal lattice unit was oriented along the Y axis. This allows us to easily calculate the lattice constant once the L_y dimension was exactly known.

As described in Sect. 2.4, we compared the tangential pressures of the two phases, and if the pressure of the solid phase is greater than that in the gas phase, this means that L_y is smaller than it should be. To achieve the equality of the two tangential pressures we slightly increase L_x and L_y, and keeping the ratio $L_y/L_x = \sqrt{3}/4$.

Figure 1 presents the density distribution of argon atoms in the first molecular layer at 40 K, with 250 molecules in this layer. The contour plot shown in Fig. 1 is a density of probability of finding a molecule at any point of the XY plane. This representation is more informative than the snapshot because it is a result of averaging over a large number of kMC steps (5×10^7 in the case under consideration). If the distribution were uniform, the density would be unity over the whole monolayer. The maximum density for the case presented in Fig. 1 is 35. Such a high probability density

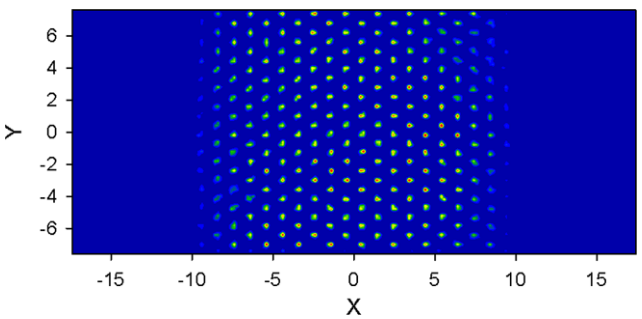

Fig. 1 Density distribution of argon adsorbed on graphite at 40 K simulated with *kMC* in canonical ensemble. The simulation box lengths L_x, L_z are 34.67 and $10\sigma_{ff}$, respectively. $L_y = L_x 3^{1/2}/4$. The number of molecules $N = 250$. Color changes from *blue* at zero to *red* for $\rho^* = \rho\sigma_{ff}^3 = 25$ according to the rainbow scheme of color

means that the hexagonal structure of the monolayer is very stable and the gas–solid interface is quite sharp. As seen in Fig. 1, there are 13 unit cells of the lattice along the L_y direction, which gives a lattice constant of $L_y/13$.

Figure 2 shows the dependence of the lattice constant l on temperature.

The lattice constant increases with temperature due to the increase of mobility of molecules, for the range of temperatures tested the lattice constant is greater than the distance between a pair of molecules at which the potential of interaction is minimal. This means that if the molecules were situated exactly at the apexes of a perfect hexagonal lattice each molecule would experience attraction from neighboring molecules, resulting in a negative tangential pressure.

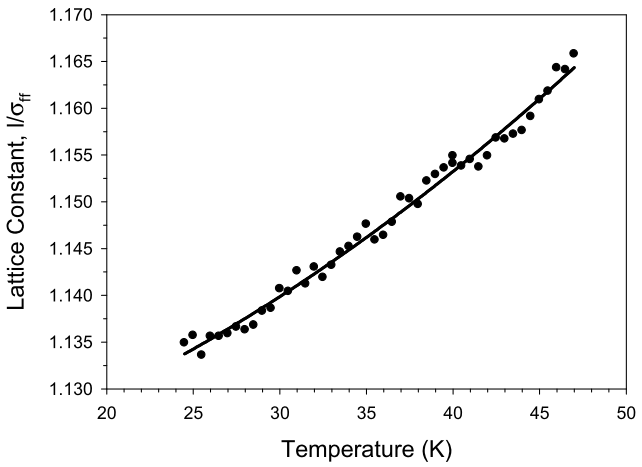

Fig. 2 Lattice constant of a hexagonally packed argon monolayer adsorbed on graphite. $L_y = L_x 3^{1/2}/4$. The number of molecules $N = 250$

However, due to the thermal motion the pressure is positive because it must be equal to the tangential pressure in the coexisting gas phase.

On the other hand, at temperatures below the melting temperature the tangential pressure is very small because it is the same as that of the highly rarefied coexisting gas, so the dimensionless value $\xi_j = p_T V/(jk_BT)$ is close to zero. This gives a recipe how to choose the size of the simulation box at a low temperature to model a completed uniform monolayer at a point when the number of molecules j coincides with the number of unit cells of the 2D hexagonal lattice. Thus, if one takes $j = 400$ and adjusts the length L_x so that the time average of ξ_j is close to zero, the lattice constant would be $L_x/20$ because 20×20 is the number of unit cells. We have tested this technique for 40 K as follows. Initially we achieved the equilibrium state for 400 molecules at 40 K in the simulation box having length $L_x = 23\sigma_{ff}$. Then we ran kMC simulation for 2×10^8 MC steps divided into 200 cycles. In each cycle of 1×10^6 MC steps we determined the time average value of ξ_j. If this value was less than zero, the length L_x was decreased by $0.0005\sigma_{ff}$, and *vice versa*. As a result, the value $L_x = 23.08\sigma_{ff}$ was obtained, which corresponds to the lattice constant $l = 1.154\sigma_{ff}$ or 0.3916 nm. This value exactly coincides with the fitting curve at 40 K presented in Fig. 2. The size of the box determined by this method can be used as an initial value for simulation of the adsorption isotherm and thermodynamic functions with the variable box size. The isotherm and the heat of adsorption simulated at 40 K are shown in Fig. 3. As seen in Fig. 3a, once the monolayer has been completed, the addition of a small amount of adsorbate leads to sharp increase of the specific amount adsorbed because of the contraction of the lattice. It can be explained as follows. The

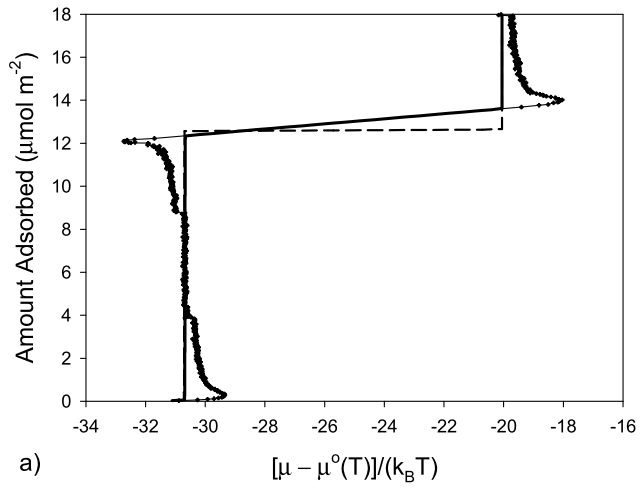

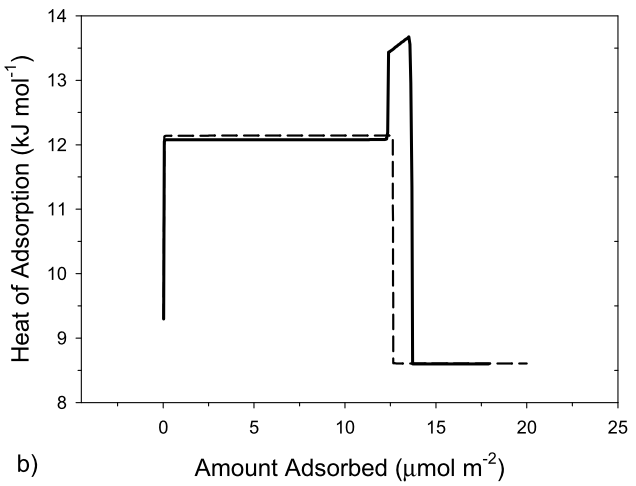

Fig. 3 Adsorption isotherm of Ar at 40 K (**a**) and the isosteric heat of adsorption (**b**) simulated with the kMC in the box of varied size (*solid lines*). *Dashed lines* are simulated in the box of constant size with the length $L_x = 23\sigma_{ff}$. *Points* correspond to the adsorption isotherm simulated in canonical ensemble. The *thick solid line* (**a**) is plotted with Eq. (9)

addition of only one molecule to the system makes an insignificant change in the molecular Helmholtz free energy, but this extra molecule resides in the second layer and due to much lower interaction with the substrate and neighboring molecules it has much larger mobility than any molecule in the first monolayer. For this reason, this extra molecule significantly contributes to the chemical potential, which jumps toward higher value by more than 10 $k_B T$. However, as far as the system obeys equilibrium thermodynamics, the specific Helmholtz free energy is the difference between the chemical potential μ and $p_T V/j$, where j is the total number of molecules. In order to retain the same Helmholtz free energy it is necessary to sharply increase the tangential pressure correspondingly to the change of the chemical potential. This is possible only by contraction of the monolayer and the decrease in the lattice constant.

The adsorption isotherm plotted with points in Fig. 3a is computed with the canonical kMC accounting for the change of the box size according to the scheme based on the Gibbs–Duhem equation and described in Sect. 2.1. The solid line with vertical transition steps is plotted with Eq. (9). Note that the position of the first vertical step coincides with that of the canonical isotherm corresponding to splitting of the adsorbed argon into coexisting gas and 2D solid. For comparison, the adsorption isotherm simulated in the box of specified size and then treated with Eq. (9) is plotted by the dashed line. One can see that the use of the box of constant size leads to significant errors. In this context it is interesting to consider the differential heat of adsorption presented in Fig. 3b. The standard technique in the box of constant size leads to a simple behavior of the adsorbed phase. First, the heat of adsorption jumps to the value 12.14 kJ/mol which is the heat of the gas solid transition accounting for the argon–graphite interaction. Once the first monolayer is completed, the heat of adsorption drops to 8.6 kJ/mol. This is the gas–solid transition in the second layer and the difference is due to the difference of the adsorption potential in these layers. However, the thermodynamically consistent model results in the appearance of the narrow peak in the heat curve just after the completion of the first monolayer which is due to release of additional energy resulting from the contraction of the adsorbed layer.

3.2 Gas–liquid coexistence of argon in the adsorbed monolayer

Vapor–liquid equilibrium was analyzed with the same method used for the gas–solid coexistence except the region close to the critical temperature. The density probability distribution in the monolayer at 50 K is presented in Fig. 4.

Comparing Fig. 1 for the case of 2D vapor–solid equilibrium and Fig. 4 for this case of 2D vapor–liquid equilibrium at 50 K we can see that in the latter case the monolayer

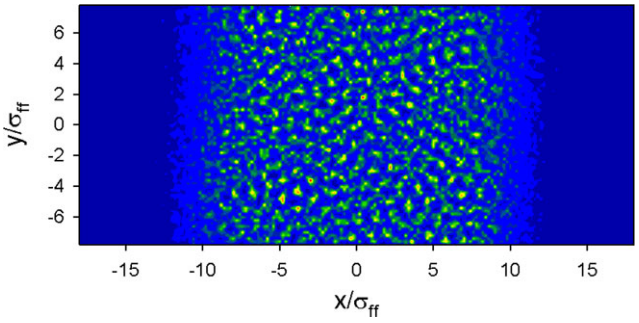

Fig. 4 Density probability distribution of argon adsorbed on graphite at 50 K simulated with *kMC* in canonical ensemble. The simulation box lengths L_x, L_z are 36.0 and $10\sigma_{ff}$, respectively. $L_y = L_x 3^{1/2}/4$. The number of molecules $N = 250$. Color changes from *blue* at zero to *red* for $\rho^* = 9.92$ according to rainbow scheme of color

structure is disordered, though some hexagonal patterns are visible. This means that 50 K is above the 2D triple point. For a disordered structure the size of the simulation box is not critical, therefore we have carried out simulations of the gas–liquid coexistence with $L_x = 36\sigma_{ff}$.

The phase diagram is shown in Fig. 5a in which results from the modeling of the gas–solid and the gas–liquid equilibrium are shown as half-filled circle symbols while the square symbols are obtained from the analysis of canonical adsorption isotherms presented in Fig. 5b for the region near the 2D-critical point. Solid lines are plotted with Eq. (9) based on the grand canonical distribution, for which the adsorption isotherms simulated in a canonical ensemble are transformed into adsorption isotherms corresponding to an ensemble of open systems. The vertical transition step on each adsorption isotherm defines the chemical potential of the 2D gas–liquid coexistence, and the densities of the coexisting phases are determined at the intersection of the vertical line with the canonical adsorption isotherm.

The densities of the coexisting phases derived from those adsorption isotherms are close to those obtained directly in the modeling of vapor–liquid equilibrium. The critical temperature is found to be 63 K, at which the canonical and grand canonical adsorption isotherms coincide and the canonical isotherm has an infinite slope at its inflection point.

The main feature of the phase diagram presented in Fig. 5a is the sharp decrease of the density of the condensed phase at 47.2 K. This temperature can be identified as the 2D-triple point for argon adsorbed on structure-less graphite. Formally, this value coincides with the temperature of the first peak on the heat capacity curve obtained by Migone et al. (1984), but as we have mentioned earlier, this temperature corresponds to the rotational transition due to the periodic modulation of the graphite potential which we do not account for in this study. In reality the melting temperature is slightly higher by 2 degrees. It is worthwhile to consider in more detail the role of surface corrugation and

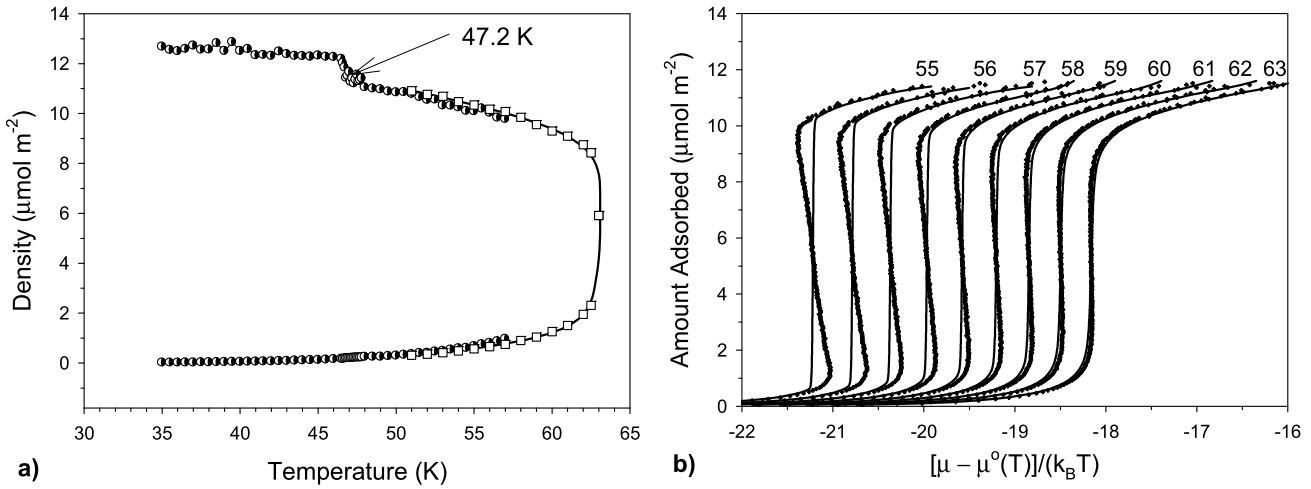

Fig. 5 (**a**) Phase diagram for argon monolayer adsorbed on graphite. *Circles* are plotted with the model simulated the gas–solid and the gas–liquid equilibrium. *White squares* are plotted with argon adsorption isotherms. The drop of density at 47.2 K corresponds to melting of the 2D crystalline monolayer. (**b**) Argon adsorption isotherms at temperatures (numbers at curves) close to the two-dimensional critical temperature. The slope of adsorption isotherms simulated in a canonical ensemble (*points*) below the critical point is negative. At the critical temperature the slope of the isotherm at a loading of about half monolayer becomes vertical. This shows that the critical temperature is close to 63 K

edge effects on the phase transition of a monolayer, and this will be a subject of our future communication. The density change at the 2D-triple point is 1.2 μmol/m^2, which is 10 % of the solid-like phase density.

3.3 Ordering transition

Simulation of the ordering transition is more involved and requires greater care because the densities of the ordered and disordered phases at equilibrium do not differ significantly, which results in a large transition zone between these phases. Therefore, it is necessary to simulate the ordering transition in a very large simulation cell. An effective alternative way is based on the careful analysis of adsorption isotherms. We simulated argon adsorption isotherms on graphite in a canonical ensemble carefully at various temperatures with an increment of one molecule for each equilibrium point. The number of MC steps for the equilibration and sampling stages were 2×10^7 and 5×10^7, respectively. The dimensions L_x was $23\sigma_{ff}$, with $L_y = (\sqrt{3}/2)L_x$, so the number of sites of the perfect hexagonal lattice in the XY plane was 400. The dimension L_z was $10\sigma_{ff}$. In order to avoid the appearance of dislocations and defects in the lattice when the ordered phase formed from the disordered phase, we started from an ordered phase and decreased the number of molecules by one. We proceeded from the assumption that if the ordering is thermodynamically favorable, random crystalline defects and dislocations disappear by themselves because it is accompanied by a decrease of the Helmholtz free energy, but it takes too much computation time. For this reason, molecules in the first monolayer were initially packed in a perfect hexagonal lattice, with the total number of molecules exceeding the number of lattice sites in the monolayer. As molecules are progressively removed from the simulation box, holes or defects are formed in the first layer with a possible rotation of the lattice. Eventually, the ordered structure disappeared.

Some selected adsorption isotherms simulated with kinetic Monte Carlo scheme are presented in Fig. 6a. As seen in Fig. 6a, the ordering transition occurs below and above the critical temperature of 63 K, but does not occur below the 2D triple point of 47.2 K. At 40 K, which is below the triple point, the formation of the ordered monolayer occurs due to the gas–solid transition and there is no ordering transition of the solid phase.

The ordering transition can also be measured with a statistical order parameter. In this paper, we used the bond-orientational Ψ_6 parameter (Strandburg 1988):

$$\Psi_6 = \frac{1}{N_b} \sum_j \sum_k \cos(6\phi_{jk}) \tag{19}$$

where N_b is the number of bonds between nearest molecules, ϕ_{jk} is the angle between the bond connecting molecules j and k and an arbitrary reference axis. The first sum runs over all molecules and the second sum runs over all nearest neighbors of the molecule j.

Figure 6b presents the order parameter versus loading at various temperatures from 40 to 77 K. At 40 K which is below the melting point the order parameter is relatively high for loadings below and above the monolayer completion. This means that a crystalline phase exists even at coverages

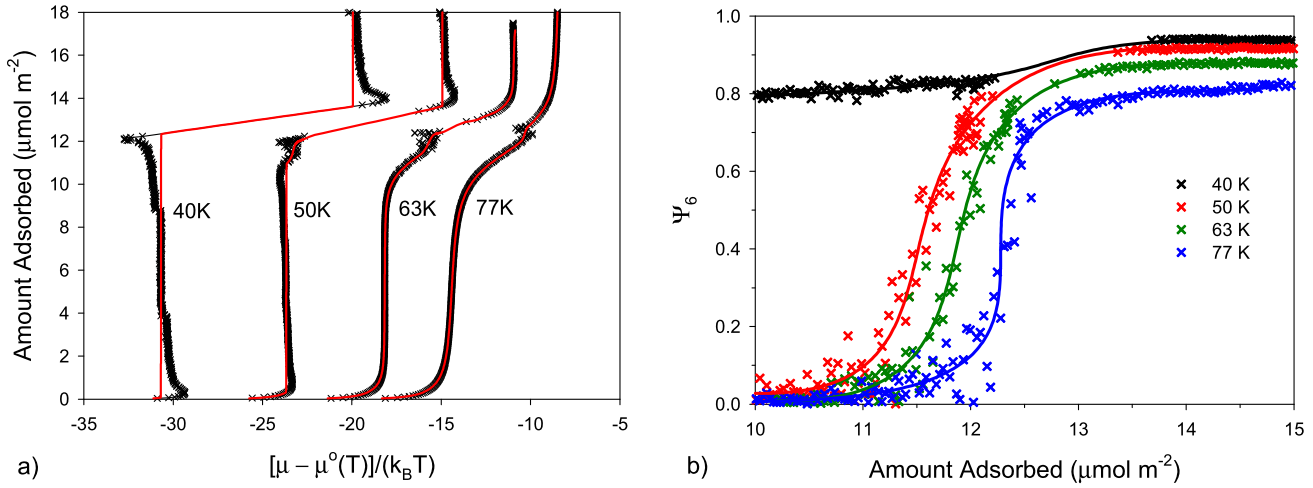

Fig. 6 (**a**) Argon adsorption isotherms on the graphite simulated in a canonical ensemble (*crosses*) with kMC at 40, 50, 63, and 77 K. *Red lines* are plotted with (9) and refer to an ensemble of open systems. (**b**) The order parameter versus loading

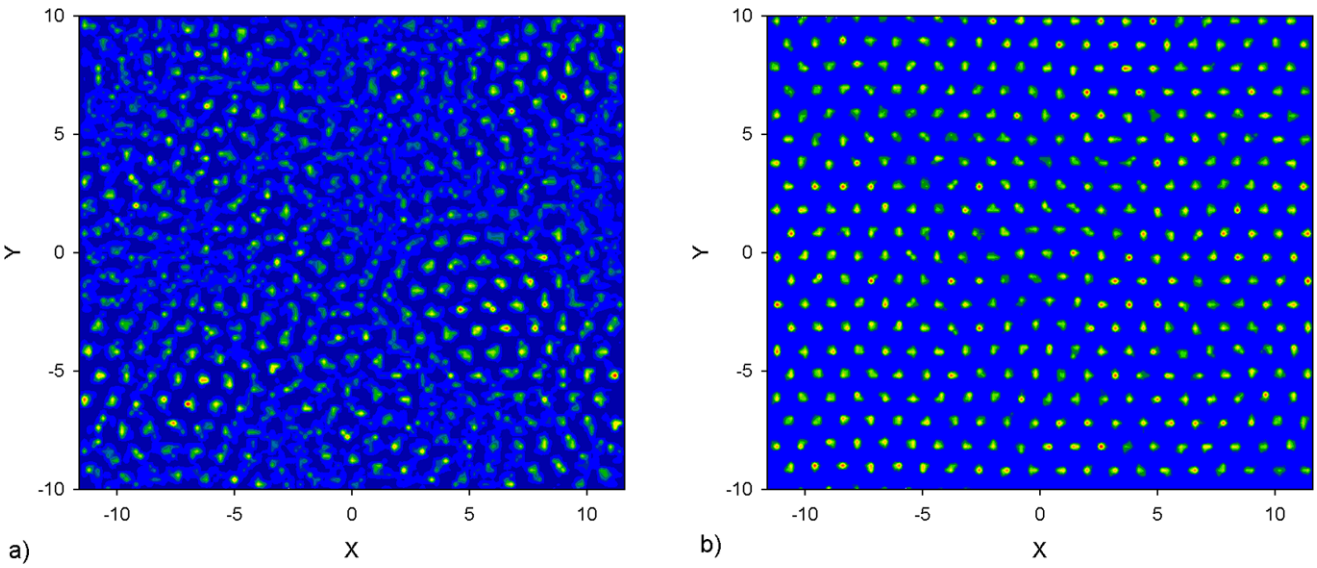

Fig. 7 Density distribution of argon monolayer on graphite at 77 K before (**a**) and after (**b**) the ordering transition. The amount adsorbed is 11.93 (**a**) and 12.46 μmol/m^2 (**b**)

less than the monolayer concentration, and it coexists with the 2D gas phase. At temperatures greater than the melting temperature a 2D crystal-like phase forms as a consequence of a high tangential pressure at a loading close to the monolayer coverage. In this case a decrease of the entropy due to a molecular ordering is compensated by a more significant decrease of the internal energy followed by a decrease of the Helmholtz free energy, which facilitates the ordering transition. An illustration of this process at 77 K is presented in Fig. 7.

As seen in Fig. 7a, at the stage just preceding the ordering transition the monolayer consists of disordered fraction and hexagonally ordered domains. The increase of the amount adsorbed by 0.5 μmol/m^2, i.e. by 4 % results in appearance of a defect free hexagonally ordered 2D phase (Fig. 7b).

Adsorption isotherms as well as the internal energy versus loading simulated at various temperatures allow the isosteric heat of adsorption to be calculated, which gives additional information on the mechanism of adsorption.

3.4 Heat of adsorption

Calculation of the isosteric heat of adsorption was made with Eq. (13). Figure 8 shows the heat of adsorption at various temperatures.

Similar trend of the evolution of the heat curve versus loading was reported in the literature (Do et al. 2008;

Nguyen et al. 2010), using a grand canonical simulation, but the accuracy of the heat curve in this figure is much better with the method presented in this paper.

As seen in Fig. 8, the behavior of the heat of adsorption versus loading substantially changes with temperature. Below the 2D triple point the heat of adsorption is constant from very low loading to the completion of the monolayer. This is the heat of solidification. When the second monolayer starts to form, the heat of adsorption increases and then drops to a smaller value, but is constant until the second layer is completed. At 50 K, which is 2.8 K above the 2D-triple point the heat curve drastically changes. Instead of the gas–solid transition as observed with temperatures below the 2D-triple point, we see the gas–liquid transition at a lower heat of adsorption, decreasing from 12.14 to 11.69 kJ/mol, a drop by 0.45 kJ/mol. However, at a higher loading the ordering transition has occurred resulting in the same hexagonal two-dimensional structure as if it were solidification. Surprisingly, the heat of the ordering transition is 15.6 kJ/mol, which is markedly larger the heat of the gas–solid transition. The difference is 3.5 kJ/mol, which is resulted from the reorganization of existing molecules in the first layer to form hexagonal lattice and the increase of its surface density during ordering. At 50 K there is an additional peak after the completion of the first monolayer provided by the contraction of the monolayer.

At the 2D critical temperature (the green line in Fig. 8) the vapor–liquid transition does not occur and therefore the heat curve is monotonic up to the ordering transition. The onset of the ordering occurs at a higher loading, and the heat of this transition is again larger than that at 40 K because of the greater organization of the existing molecules in the first layer and its larger capacity than that of the disordered layer. The second heat spike due to the densification of the monolayer after its completion is still seen, but it is less pronounced and overlaps with the main heat spike associated with the ordering transition. At 77 K, which is a 2D-supercritical temperature a new feature has appeared. A drop of the heat of adsorption (cusp) preceding the heat spike is observed on the heat curve, and the maximum of the heat spike achieves 15.8 kJ/mol. The second spike induced by the monolayer densification has disappeared.

A relatively high heat of the ordering transition corroborates our argument to distinguish it from the melting/freezing transition. This interesting phenomenon needs further investigations over a wider temperature range and accounting for the change of the lattice constant with temperature. The effect of the lattice constant change diminishes at relatively higher temperatures. This suggests that the heat of adsorption can be simulated with a specified, but appropriately chosen simulation box size. Thus, we used the dimension L_x of $23\sigma_{ff}$, which corresponds to the lattice constant $l = 1.15\sigma_{ff}$. As is known from our previous work (Ustinov and Do 2012b) this value is close to that corresponding to the onset of the ordering transition at the point of completion of the first monolayer. Further increase of the amount adsorbed decreases the lattice constant, but the heat spike is reproduced correctly at the above value because the heat of ordering releases before the lattice constant has changed significantly.

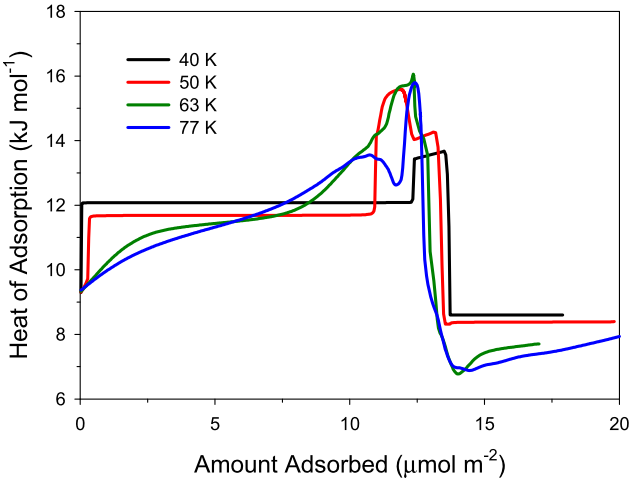

Fig. 8 Isosteric heat of argon adsorption on graphite at 40, 50, 63, and 77 K

Figure 9a presents the segments of adsorption isotherms in the neighborhood of the disorder–order transition for a narrower temperature interval from 77 to 88 K, and the corresponding heats of adsorption are shown in Fig. 9b.

As seen in Fig. 9, the ordering transition exists even at 88 K, which is slightly above the argon boiling point. The solid lines correspond to an ensemble of open systems and are plotted with (9). The kink on the isotherms (solid lines in Fig. 9a) which corresponds to the ordering transition is clearly seen at 77 to 82 K. At 88 K it is masked by formation of the second molecular layer, but the ordering transition still exists at this temperature. This is confirmed by heat curves (Fig. 9b) each of which has a prominent heat spike. The spike shifts to higher loadings and the maximum in those spikes decreases as temperature is increased. Interestingly, the magnitude of jump at the spike increases with temperature. At temperatures greater than 88 K we were unable to model an ordered structure of the adsorbed monolayer, suggesting that the 2D critical temperature of the 2D ordering transition is close to 88 K. This is corroborated by the coordination number and the monolayer capacity versus temperature shown in Fig. 10. The coordination number was calculated as the average number of neighbors of a given molecule within the distance of $1.4\sigma_{ff}$ in the XY plane. This gives a value which is reasonably close to that determined by the integration of the 2D radial distribution function with respect to the radial distance from zero to its first minimum.

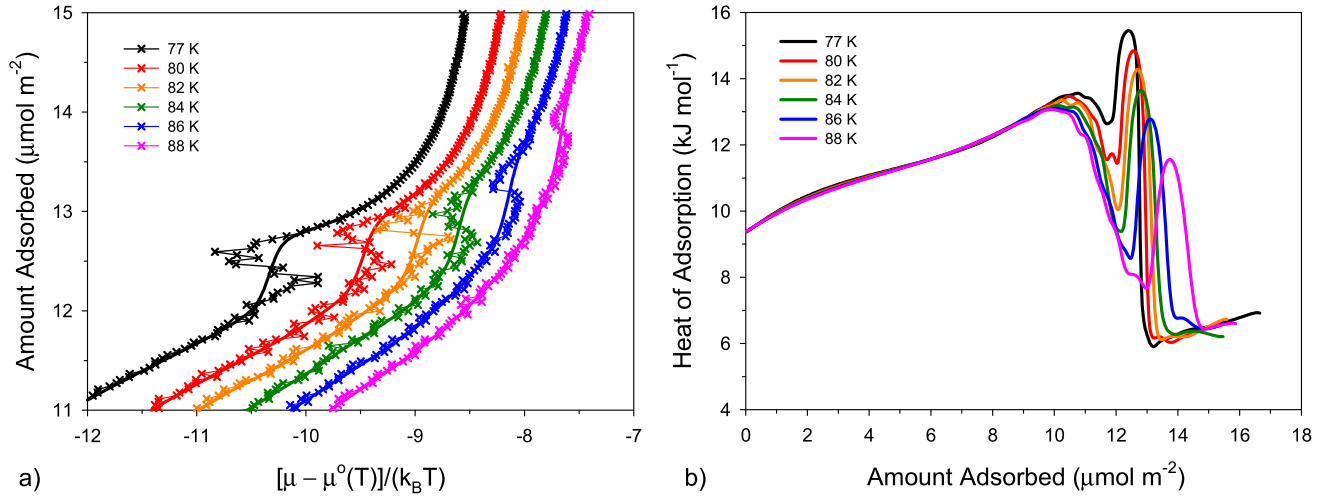

Fig. 9 Argon adsorption isotherms (**a**) simulated with kMC and corresponding isosteric heat of adsorption (**b**). *Points* are obtained in canonical ensemble. *Smoothed solid lines* are plotted with Eq. (9). Isosteric heat curves are calculated by (13)

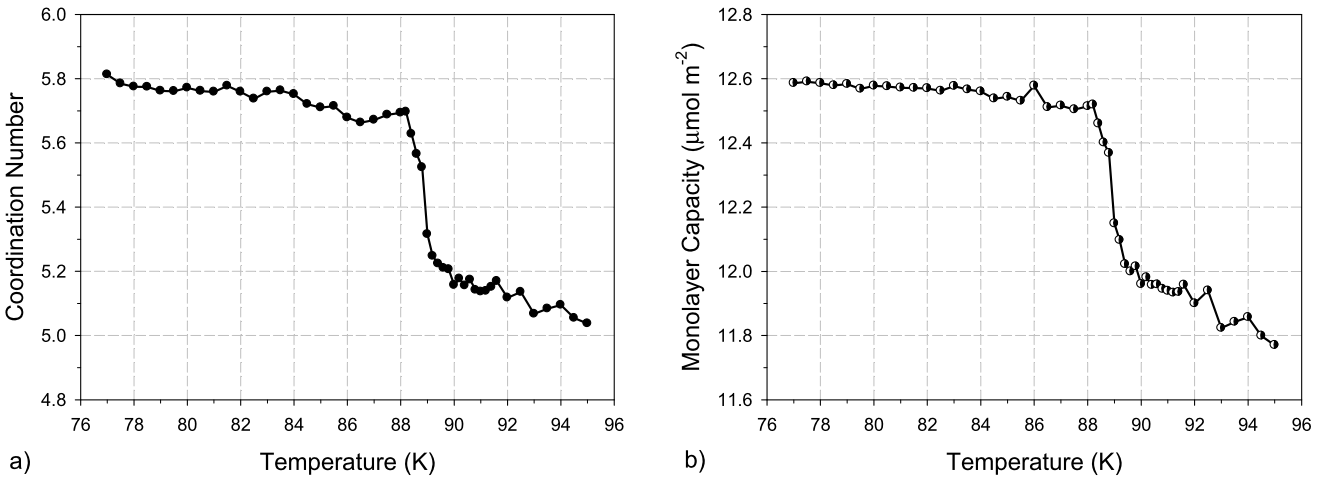

Fig. 10 Coordination number (**a**) and monolayer capacity (**b**) versus temperature for argon adsorbed on graphite. The coverage is 1.125, i.e. 450 molecules in the box with 400 molecules constituting the defect free hexagonal layer. The simulation box lengths L_x, L_z are 23 and $10\sigma_{ff}$, respectively. $L_y = L_x 3^{1/2}/2$

The coordination number of the argon monolayer is relatively large below 89 K and close to the upper limit of 6 for a 2D layer, which indicates that the adsorbed argon is ordered and forms a hexagonal structure. At 89 K the coordination number sharply decreases, suggesting that an ordered structure cannot be maintained at temperatures greater than 89 K. The same conclusion can be derived from the dependence of the monolayer capacity on temperature. The order–disorder transition leads to a decrease of the 2D density, and, consequently, to a decrease of loading. Therefore, the structure of the adsorbed monolayer of argon is disordered at temperatures greater than 89 K, and this temperature can be identified as the critical temperature of the 2D order–disorder transition.

3.5 The lattice constant correction

In order to correct the simulation box size and, consequently, the lattice constant using the Gibbs–Duhem equation (5) it is necessary to integrate the adsorption isotherm over all previously determined points, i.e. the size of the box, tangential pressure and chemical potential at N molecules in the system can be determined if these variables are known at $(N-1)$ molecules. Of course, it would be preferable to have a method that allows for determination all thermodynamic properties of the adsorbed phase including the lattice constant directly without recourse to a sequential computation of thermodynamic functions along the adsorption isotherm. However, it seems to be hardly possible because in case of formation of an ordered structure the boundary

conditions chosen arbitrarily violate the system and change its thermodynamic properties relative to the corresponding macroscopic phase. This means that boundary conditions imposed on the system with incorrectly chosen simulation box size create an artificial system which can be thermodynamically self-consistent but differs from a very large box where boundary conditions do not play a significant role. The thermodynamic consistency of a system can be easily checked using, for example, the following equation derived from the First law of thermodynamics at constant number of molecules:

$$\frac{\partial U}{\partial V} = T^2 \frac{\partial (p_T/T)}{\partial T} \tag{20}$$

where U is the internal energy and V is the volume of the simulation box. Since we change the volume of the simulation box at the same length L_z, only tangential pressure appears in the RHS of (20). We have stated that Eq. (20) is satisfied reasonably well at *any* size of the simulation box regardless whether the monolayer is ordered or disordered. This means that there is not any internal criterion of finding the box size at which the effect of boundary conditions on the system properties disappears. Nevertheless, the method based on integration of the Gibbs–Duhem equation is more effective and takes less computational resources than that based on searching the point of equality of the virial and thermodynamic pressure on adsorption isotherms simulated in boxes of different size (Ustinov and Do 2012b).

Figure 11 presents the length L_x of the simulation box versus loading at various temperatures determined by integration of the Gibbs–Duhem equation in the form of Eq. (4). The lattice constant is $L_x\sigma_{ff}/20$ because one axis of the hexagonal lattice was kept parallel X axis.

As seen in Fig. 11, the box size significantly changes, especially at low temperatures and loadings slightly above the monolayer coverage. Each curve passes through several hundred points along the adsorption isotherm without a smoothing procedure. For this reason some fluctuation along each curve is visible due to the fluctuation of the tangential pressure and the chemical potential determined in the *kMC* scheme. The points plotted in Fig. 11 are determined at 77 K with the method developed previously (Ustinov and Do 2012b). The box size used in our previous work was smaller than that used in the present study and the number of molecules in the complete hexagonally packed monolayer was 256 compared to 400 molecules in this work. Therefore, the length L_x determined previously was corrected by a multiplier 20/16. As a result, these points perfectly coincide with the dependence calculated at the same temperature with the new method using integration of the Gibbs–Duhem equation, which confirms the concept of strong interrelation between the lattice constant of an ordered adsorbed molecular layer and loading and temperature.

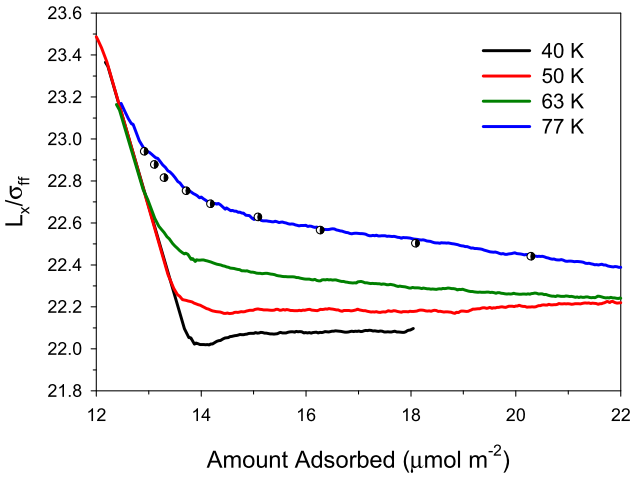

Fig. 11 Change of the length L_x of the simulation box with loading at various temperatures calculated with the Gibbs–Duhem equation in the system Ar–graphite. $L_y = L_x 3^{1/2}/2$. $L_z = 10\sigma_{ff}$. *Points* are plotted for 77 K with the method described previously (Ustinov and Do 2012b)

The present study again elucidates the importance of a correct choice of simulation box for a thermodynamically correct simulation of adsorption isotherms in those cases when an ordering transition occurs in the monolayer. This study should be continued in order to reveal the effects of the ordering transition in case of more complex molecules, surface corrugation, surface defects and functional groups, etc. It is also important to extent this methodology to adsorption in pores, especially in micropores which could lead to a more robust method of characterization of porous structure of various materials.

4 Conclusion

We analyzed the thermodynamics of gas–solid, gas–liquid and the ordering transition of sub- and supercritical fluid adsorbed in the monolayer on the graphite surface using the kinetic Monte Carlo scheme, which has been recently adapted successfully for equilibrium systems. It is shown that over a wide range of temperatures above the two-dimensional triple point there is a heat spike on the heat curves versus loading and the spike is an indication of the disorder–order transition. It is found that the heat of the ordering transition substantially exceeds the heat of the 2D gas–solid transition at temperatures below the 2D triple point. In cases where the monolayer has an ordered structure, it is essential and vital to account for the dependence of the lattice constant of the ordered structure on loading and temperature; otherwise the simulated adsorption isotherm would be thermodynamically incorrect. To this end, we proposed a new method of accounting the dependence of the lattice constant and, consequently, an adaptive method of correcting the simulation

box size in order to achieve thermodynamically consistent results. This allows for establishing an additional effect of the heat release at temperatures below the 2D critical point resulted from the sharp densification of the crystalline lattice with loading just after the completion of the monolayer. It is an interesting task to confirm this theoretical prediction experimentally.

Acknowledgements This work is supported by Russian Foundation for Basic Research (project No 11-03-00129-a). Support from the Australian Research Council is also acknowledged.

References

Abraham, F.: The phases of two-dimensional matter, their transitions, and solid-state stability: a perspective via computer simulation of simple atomic systems. Phys. Rep. **80**, 339–374 (1981)

D'Amico, K.L., Bohr, J., Moncton, D.E., Gibbs, D.: Melting and orientational epitaxy in argon and xenon monolayers on graphite. Phys. Rev. B **41**, 4368–4376 (1990)

Day, P., Lysek, M., Madrid, M., Goodstein, D.: Phase transitions in argon films. Phys. Rev. B **47**, 10716–10726 (1993)

Do, D.D., Nicholson, D., Do, H.D.: On the anatomy of the adsorption heat versus loading as a function of temperature and adsorbate for a graphitic surface. J. Colloid Interface Sci. **325**, 7–22 (2008)

Fan, Ch., Birkett, G., Do, D.D.: Effects of surface mediation on the adsorption isotherm and heat of adsorption of argon on graphitized thermal carbon black. J. Colloid Interface Sci. **342**, 485–492 (2010)

Fan, Ch., Razak, M.A., Do, D.D., Nicholson, D.: On the identification of the sharp spike in the heat curve for argon, nitrogen, and methane adsorption on graphite: reconciliation between computer simulations and experiments. J. Phys. Chem. C **116**, 953–962 (2012)

Flenner, E., Etters, R.D.: Behavior of partial monolayers of argon adlayers deposited on graphite. Phys. Rev. Lett. **88**, 106101 (2002)

Flenner, E., Etters, R.D.: Properties of argon adlayers deposited on graphite from Monte Carlo calculations. Phys. Rev. B **73**, 125419 (2006)

Golebiowska, M., Firley, L., Kuchta, B., Fabianski, R.: Structural transformations of nitrogen adsorbed on graphite: Monte Carlo studies of spatial heterogeneity in multilayer system. J. Chem. Phys. **130**, 204703 (2009)

Grillet, Y., Rouquerol, F., Rouquerol, J.: Two-dimensional freezing of nitrogen or argon on differently graphitized carbons. J. Colloid Interface Sci. **70**, 239–244 (1979)

Hansen, J.P., McDonald, I.R.: Theory of Simple Liquids, 2nd edn. Academic Press, London (1986)

Irving, J.H., Kirkwood, J.G.: The statistical mechanical theory of transport processes. IV. The equations of hydrodynamics. J. Chem. Phys. **18**, 817 (1950)

Kuchta, B., Etters, R.D.: Calculated properties of monolayer and multilayer N_2 on graphite. Phys. Rev. B **36**, 3400–3406 (1987)

Larese, J.Z., Zhang, Q.M.: Phase transitions of argon multilayer films on graphite: evolution from multilayer film to bulk solid. Phys. Rev. B **51**, 17023–17027 (1995)

Migone, A.D., Li, Z.R., Chan, M.H.W.: Melting transition of submonolayer Ar adsorbed on graphite. Phys. Rev. Lett. **53**, 810–813 (1984)

Morrison, J.A.: Calorimetry in the study of physical adsorption. Pure Appl. Chem. **59**, 7–14 (1987)

Nguyen, V.T., Do, D.D., Nicholson, D.: On the heat of adsorption at layering transitions in adsorption of noble gases and nitrogen on graphite. J. Phys. Chem. C **114**, 22171–22180 (2010)

Nicholson, D., Parsonage, N.G.: Simulation studies of the fluid–solid monolayer transition in argon adsorbed on graphite at 77.5 K. J. Chem. Soc. Faraday Trans. **2. 82**, 1657–1667 (1986)

Nicholson, D., Rowley, L.A., Parsonage, N.G.: Monte Carlo calculations for the interaction of 12-6 argon at 80 K with graphite in the region of monolayer adsorption. J. Phys. **38**, 69–75 (1977)

Pettersen, M.S., Lysek, M.J., Goodstein, D.L.: Melting in monolayer adsorbed films. Phys. Rev. B **40**, 4938–4946 (1989)

Rouquerol, J., Partyka, S., Rouquerol, F.: Calorimetric evidence for bidimensional phase change in the monolayer of nitrogen or argon adsorbed on graphite at 77 K. J. Chem. Soc. Faraday Trans. I **73**, 306–314 (1977)

Strandburg, K.J.: Two-dimensional melting. Rev. Mod. Phys. **60**, 161 (1988)

Thomy, A., Duval, X.: Adsorption de molecules simples sur graphite. J. Chim. Phys. **67**, 286–290 (1970)

Ustinov, E.A., Do, D.D.: Two-dimensional order–disorder transition of argon monolayer adsorbed on graphitized carbon black: kinetic Monte Carlo method. J. Chem. Phys. **136**, 134702 (2012a)

Ustinov, E.A., Do, D.D.: Thermodynamic analysis of ordered and disordered monolayer of argon adsorbed on graphite. Langmuir **28**, 9543–9553 (2012b)

Ustinov, E.A., Do, D.D.: Application of kinetic Monte Carlo method to equilibrium systems: vapor–liquid equilibria. J. Colloid Interface Sci. **366**, 216–223 (2012c)

Ustinov, E.A., Do, D.D.: Simulation of gas adsorption on a surface and in slit pores with grand canonical and canonical kinetic Monte Carlo methods. Phys. Chem. Chem. Phys. **14**, 11112–11118 (2012d)

Wongkoblap, A., Do, D.D.: Explanation of the unusual peak of calorimetric heat in the adsorption of nitrogen, argon and methane on graphitized thermal carbon black. Phys. Chem. Chem. Phys. **10**, 1106–1113 (2007)

Zhu, D.M., Dash, J.G.: Surface melting and roughening of adsorbed argon films. Phys. Rev. Lett. **57**, 2959–2962 (1986)